Macromolecules

Article

Cite This: Macromolecules 2018, 51, 6327−6333

pubs.acs.org/Macromolecules

Universal Knot Spectra for Confined Polymers

Liang Dai[†] and Patrick S. Doyle*[,†,‡]

[†]BioSystems and Micromechanics IRG, Singapore-MIT Alliance for Research and Technology Centre, Singapore 117543

[‡]Department of Chemical Engineering, Massachusetts Institute of Technology (MIT), Cambridge, Massachusetts 02139, United States

Supporting Information

ABSTRACT: Knotting is a prevalent phenomenon which occurs at the macroscale (e.g., in headphone cords) and at the microscale (e.g., in DNA and proteins). For a confined polymer, the knotting probability can rapidly approach 100% as the degree of confinement increases, while the mechanism of knot formation in a confined space is unclear. In this work, we use computer simulation to generate equilibrium conformations of a polymer confined in a sphere or a tube and then calculate the knotting probability, p_{knot}, and the knot complexity that is quantified by the minimal crossing number, N_{cross}. Surprisingly, we find a universal correlation between p_{knot} and $\langle N_{cross}\rangle$. Further analysis reveals that the universal correlation is caused by the fact that the distribution of knot types, i.e., the knot spectrum, of a confined polymer follows a universal behavior, only depending on the total knotting probability, regardless of the polymer length, bending stiffness, and degree of confinement. Such universal behavior reveals a possible mechanism of knot formation in a confined space via random threading of segments among other segments. The universal behaviors agree with prior experimental and simulation results of DNA knots and can be practically useful to infer $\langle N_{cross}\rangle$ from p_{knot}, or vice versa, in the case that either one is difficult to be measured.

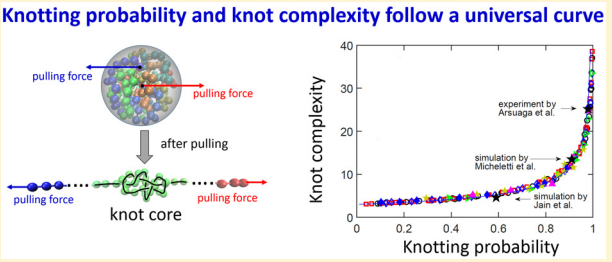

1. INTRODUCTION

Knots are pragmatic constructs which predate the discovery of fire, have been used by sailors for centuries, and pervade our everyday life.[1] Knotting is a ubiquitous phenomenon for linear objects from the macroscopic scale,[2−5] e.g., headphone cords (Figure 1a), to the microscopic scale, e.g., actin filaments,[6] DNA,[7] proteins,[8−10] and other polymers. Various effects of knots have been discovered, including reducing mechanical strength of polymers,[6] jamming nanopore translocation,[11] slowing down the relaxation of a compressed DNA[12] and stretching kinetics of DNA,[13] affecting DNA ejection from a capsid,[14−17] facilitating catalysis of proteins[18] and small molecules,[19] and impairing protein degradation.[20] The practical applications of knots have also been explored, such as controlling translocation speed of DNA through a nanopore for sequencing.[21,22] Knots affect the behaviors of polymers to different extents, depending on the knotting probability and knot complexity. For example, compared to a headphone cord in free space, a headphone cord taken out of a small pocket takes more time to be untied because the compression of the pocket increases the knotting probability and the knot complexity (Figure 1a). Experimental, theoretical, and simulation studies have been performed to investigate the knotting probability and the knot complexity, such as in free space,[23−29] in spatial confinement,[30−35] under pulling force,[6,7,36,37] by electric-field compression,[12,38] and with intrachain interactions.[39−41] Despite over a century of research on the topic of knots, there is no understanding of how their probability of occurrence relates to their geometric complexity.

In this paper, we report a surprising finding that the distribution of knot complexity, i.e., knot spectrum, for a confined polymer follows a universal behavior which only depends on the total knotting probability, regardless of the polymer length, bending stiffness, and degree of confinement. The universal knot spectrum leads to a universal correlation between the knotting probability and knot complexity. Such universal behavior reveals a possible mechanism of knot formation in a confined space: random combinations of the over−under statuses of apparent crossings.

2. METHODS

2.1. Generation of Confined Polymers. We first generate equilibrium conformations of single polymers confined within a sphere, a tube, or a slit using a modified PERM (pruned-enriched Rosenbluth method[42]) and then pull both ends of each conformation by force in a Brownian dynamics (BD) simulation for the purpose of classifying knots (Figure 1b). The modified PERM generates polymer conformations based on chain growth, i.e., placing a bead randomly in space and then adding beads one by one until the desired length is reached.[43] In the modified PERM, we model a polymer as a string of touching beads with three interactions: hard-core repulsion between beads with diameters of a, bending energy to produce a persistence length L_p, and hard-core repulsion between beads and the sphere or tube that confines the polymer. For each parameter set $\{L, L_p, D_{sphere}$ or $D_{tube}\}$, we generate 1000−10000 conformations.

Received: June 25, 2018
Revised: July 25, 2018
Published: August 10, 2018

DOI: 10.1021/acs.macromol.8b01340
Macromolecules 2018, 51, 6327−6333

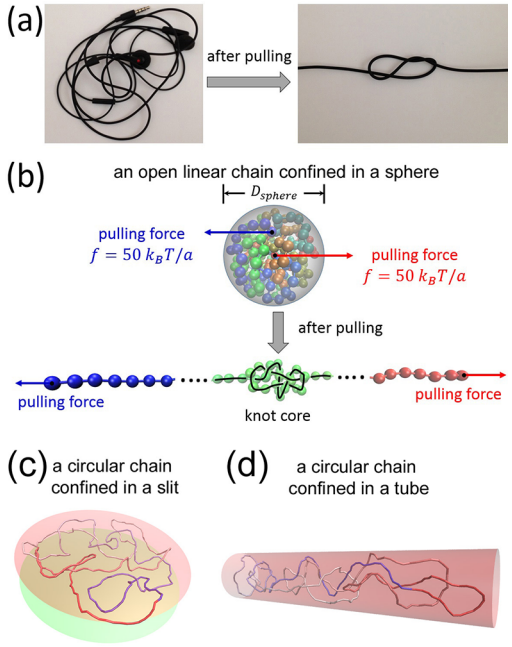

Figure 1. (a) Pulling a headphone cord to identify the knot inside. (b) The top image shows an example of a spherically confined linear polymer conformation generated by our PERM simulation with the parameters $L = 200a$, $L_p = 0$, and $D_{sphere} = 9a$. The color of beads gradually changes from blue to red along the polymer chain. We pull the first (blue) and last (red) bead of this polymer in Brownian dynamics simulation so that we can clearly observe and conveniently classify the knot core, analogous to the macroscale example in (a). In this example, the knot is 6_3, where 6 is the minimal crossing number and 3 is the index among the knots with 6 crossings. The bead size shown in images is less than the actual bead size in our simulation for better visualization. (c) A circular polymer conformation generated by our Monte Carlo simulation with the parameters $L = 300a$, $L_p = 5a$, and $H_{slit} = 5a$. (d) A circular polymer conformation generated by our Monte Carlo simulation with the parameters $L = 300a$, $L_p = 5a$, and $D_{tube} = 10a$.

The conformation generated by our modified PERM is used as the initial conformation for BD simulation using the LAMMPS package.[44] In BD simulation, there are two types of interactions: a purely repulsive Lennard-Jones potential between beads and a bond interaction for adjacent beads by a FENE potential. In addition, we apply pulling force of $f = 50\ k_BT/a$ at both ends of a polymer (Figure 1b). During BD simulations, we calculate the crossing number for the projected conformation at each step and record the minimal value among all steps, N_{cross}^{sim}. Note that N_{cross}^{sim} should be equal to or larger than the actual minimal crossing number N_{cross}^{knot} defined for a knot because trivial crossings might appear in every projected conformation during chain stretching. Our benchmark simulations of twist and torus knots demonstrate $N_{cross}^{sim} \approx N_{cross}^{knot}$ for $N_{cross}^{knot} \lesssim 50$ (see section S3 in the Supporting Information). Composite knots appear in our simulations with a probability. For composite knots, the calculated N_{cross} is the sum of N_{cross} of all prime knots. In addition to the crossing number, we also calculate the knotting probability, p_{knot}, for the confined polymer conformations.

We also use Monte Carlo simulation[29,45] to generate conformations of circular polymers within a sphere, a tube, or a slit. Analysis of knot states of these circular chains does not need to close two ends, and these results are used to confirm that our finding about knots are not caused by closing two ends.

The details of simulation methods, data analysis, and benchmark simulations can be found in the Supporting Information and our previous publications.[43,46,47] Note that confinement is necessary to explore high-p_{knot} regime in the simulation of real chains with computationally accessible lengths ($\lesssim$10000 monomers). For example, to make $p_{knot} \approx 1$, the chain length needs to be on the order of 10^6 for flexible chains with excluded volume (EV) interaction.[29]

2.2. Identification of Knots. In this study, we identify the knot types and calculate N_{cross} by two methods: (1) the calculation of Alexander polynomials and (2) the pulling process.

The first method is based on the fact that different knot types have different Alexander polynomials, except that occasionally multiple knot types share the same Alexander polynomial. We first tabulate the Alexander polynomials for 250 knot types with $0 \le N_{cross} \le 10$.[48] Then, for a given polymer conformation, we project the conformation on a plane, calculate the Alexander polynomial, and obtain the knot type through the mapping between Alexander polynomials and knot types. Note that some knots share the same Alexander polynomial; in particular, composite knots from 3_1 and 4_1 knots share the same Alexander polynomials with other prime knots. For example, the composite knots $3_1\#3_1$ and $3_1\#4_1$ share the same Alexander polynomials with 8_{20} and 8_{21} knots, respectively.[49] We always assign these overlapped Alexander polynomials to composite knots due to the following reasons. First, a previous study found that these overlapped Alexander polynomials usually correspond to the composite knots.[50] Second, we find that the probability of the overlapped Alexander polynomial between $3_1\#3_1$ and 8_{20} knots is close to the square of the probability of 3_1 knot, which supports that the overlapped Alexander polynomial comes from the $3_1\#3_1$ knot. Third, the probability of observing the overlapped Alexander polynomial between $3_1\#3_1$ and 8_{20} knots is so significant (up to a few percent) that it is unlikely from a specific prime knot 8_{20} (see section S9 in the Supporting Information). For overlapped Alexander polynomials among two or more prime knots, we assign them to the simplest knot types. Because of rare cases of overlapped Alexander polynomials and the small difference in N_{cross} among the knot types sharing one Alexander polynomial, assigning these overlapped Alexander polynomials to the most complex knot types does not make much difference in the distribution of N_{cross}. For knots with more than 10 crossing, it is impractical to determine N_{cross} through the Alexander polynomial because the number of knot types increase rapidly with N_{cross}. There are 1, 1, 2, 3, 7, 21, 49, 165, 552, 2176, 9988, 46972, 253293, and 1388705 knot types for the crossing number from 3 to 16.

The second method can estimate N_{cross} for a polymer conformation with $N_{cross} \lesssim 100$. We pull a polymer conformation in Brownian dynamics simulation using LAMMPS package.[44] We perform 10^6 to 2×10^7 steps and evenly save 1000 conformations. For these 1000 conformations, we calculate the crossing number for the projected conformation at each step and record the minimal crossing number among these 1000 conformations. Note that for each conformation we calculate the two crossing numbers for the polymer conformation projected on the two planes parallel with the pulling force and save the smaller value. The conformation projected on the plane perpendicular to the pulling force has too many crossing number and hence is not considered. Our benchmark simulations using polymer conformation with $3 \le N_{cross} \le 143$ demonstrate that the pulling method occasionally overestimates N_{cross} by a few percent, which suggests the pulling method is a reliable method for complex knots.

The results shown in this article are mostly based on the second method because we deal with complex knots with N_{cross} up to 100. We also use the first method, which is stricter, to confirm the universal behaviors in the region with $N_{cross} \le 10$.

3. RESULTS AND DISCUSSION

3.1. Knotting Probability and Knot Complexity. Figure 2 shows the knotting probability p_{knot} and the average minimal crossing number $\langle N_{cross} \rangle$ when varying the diameter of the sphere confining a polymer with $L = 300a$. We convert the spherical diameter to the volume fraction $\nu \equiv (L/a)(a/D)^3$. We find that both p_{knot} and $\langle N_{cross} \rangle$ increase with ν and L_p. Similar results were obtained previously by Micheletti et al.[51] Different from the monotonic effect of spherical

DOI: 10.1021/acs.macromol.8b01340
Macromolecules 2018, 51, 6327−6333

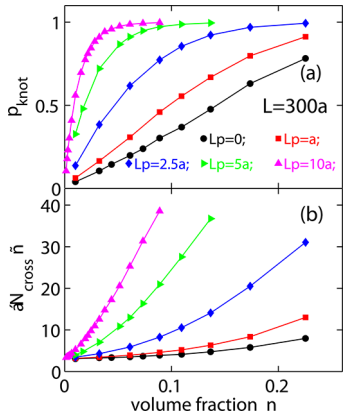

Figure 2. Knotting probability (a) and the mean value of minimal crossing numbers of knotted conformations (b) as a function of the volume fraction of linear polymer conformations in spherical confinement. The chain length is fixed at $L = 300a$. Each symbol corresponds to a different persistence length L_p.

confinement on p_{knot}, the tube and slit confinement lead to a nonmonotonic effect on p_{knot} with a maximum p_{knot} at a certain confinement strength.[33,35,52] To explore high-p_{knot} regime in tube confinement, we use tubes with closed ends to increase the compactness of polymer conformations, while the aspect ratios of tubes L_{tube}/D_{tube} are on the order of 10 or more.

3.2. Universal Correlation. On the basis of the data in Figure 2 as well as additional data for other chain lengths and tube confinement, we make a scatter plot of p_{knot} versus $\langle N_{cross}\rangle$ in Figure 3. Each data point corresponds to a simulation with a certain parameter set: L, L_p, and D_{sphere} or D_{tube}. Despite the large variation in L, L_p, D_{sphere}, and D_{tube}, surprisingly, all data points appear to follow a master curve, which indicates universal correlation between the knotting probability and the minimal crossing number. To confirm that the universal correlation is not caused by the pulling process used in our knot identification, we also analyze the knot types for $N_{cross} \leq 10$ using the Alexander polynomials. Without the pulling process, we observe the same universal correlation for linear chains (Figure 4a) and circular chains (Figure 4b). Similar results are observed from slit and tube confinement (see the Supporting Information). Recall that we use PERM simulations to generate linear polymer conformations and use Monte Carlo simulations to generate circular polymer conformations.

It is worth noting that the universal correlation (master curve) is an approximation, and small deviations from the universal correlation can be seen in Figure 3. The deviations may come from the systematic variation among different polymer parameters or from noisiness in the statistics of a limited number of polymer conformations. A trend revealed by Figure 3b is that the deviation from the universal correlation does not enlarge as N_{cross} increases. As discussed in section 3.6, the universal correlation relies on confinement and is invalid for polymers in free space. We expect that as the polymer conformations gradually vary from the free-space to weak-confinement to strong-confinement situation, the deviation from the universal correlation decreases and may eventually vanish. The data points in Figure 4 exhibit relatively large deviations because the corresponding polymer conformations experience relatively weak confinement so that the relevant knots are simple and can be identified by Alexander polynomials.

3.3. Comparison with Previous Data. The data of p_{knot} and N_{cross} measured by previous experiments and simulations fall onto this universal correlation as shown in Figure 3. Arsuaga et al.[14] obtained 97.94% DNA knots from P4 phage with $\langle N_{cross}\rangle \approx 25.2$. Micheletti et al.[51] obtained 91% knots with $\langle N_{cross}\rangle \approx 13.5$ from the simulation of a spherically confined polymer with $L = 3.4$ μm, $L_p = 50$ nm, $a = 2.5$ nm, and $D_{sphere} = 180$ nm. Jain and Dorfman[53] observed ~59% conformations containing knots and composite knots with $\langle N_{cross}\rangle \approx 4.6$ in the simulation of a channel-confined polymer with $L = 56$ μm, $L_p = 52.2$ nm, $a = 5.6$ nm, and $D_{channel} = 60$ nm.

3.4. Empirical Formula of Universal Behaviors. To estimate the functional form of the universal correlation, we make a log–log plot of $\langle N_{cross}\rangle$ versus $1 - p_{knot}$ in Figure 3b, and the data appear to be quasi-linear with a slope about 0.5 in the middle region. Accordingly, we are inspired to propose the following formula:

$$\langle N_{cross}\rangle \approx 4/\sqrt{1 - p_{knot}} - 1 \quad (1)$$

We use this formula because of its simplicity, the good fit, and its correct asymptotic behaviors: (i) $\langle N_{cross}\rangle \approx 3$ for $p_{knot} \to 0$ and (ii) $\langle N_{cross}\rangle \to +\infty$ for $p_{knot} \to 1$. The data points with $p_{knot} \gtrsim 0.96$ deviate from eq 1 but still follow a master curve.

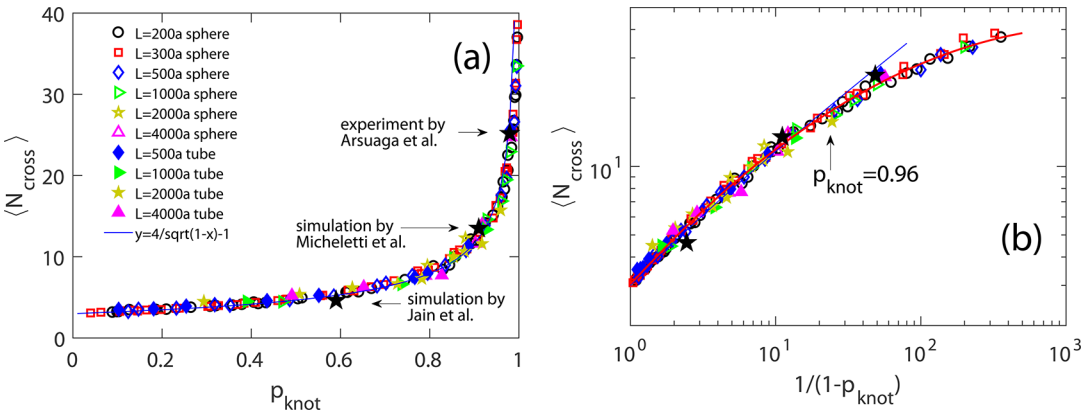

Figure 3. (a) Scatter plot of $\langle N_{cross}\rangle$ against p_{knot} when varying the linear polymer length, the persistence length, and the confinement type. We use the pulling process to estimate N_{cross}. The three black stars correspond to the data from previous experiments and simulations.[14,51,53] The blue line is from eq 1. (b) Plot of the same data, but with logarithmic scales of $\langle N_{cross}\rangle$ and $1/(1 - p_{knot})$. The blue and red lines are from eq 1 and 2, respectively.

DOI: 10.1021/acs.macromol.8b01340
Macromolecules 2018, 51, 6327–6333

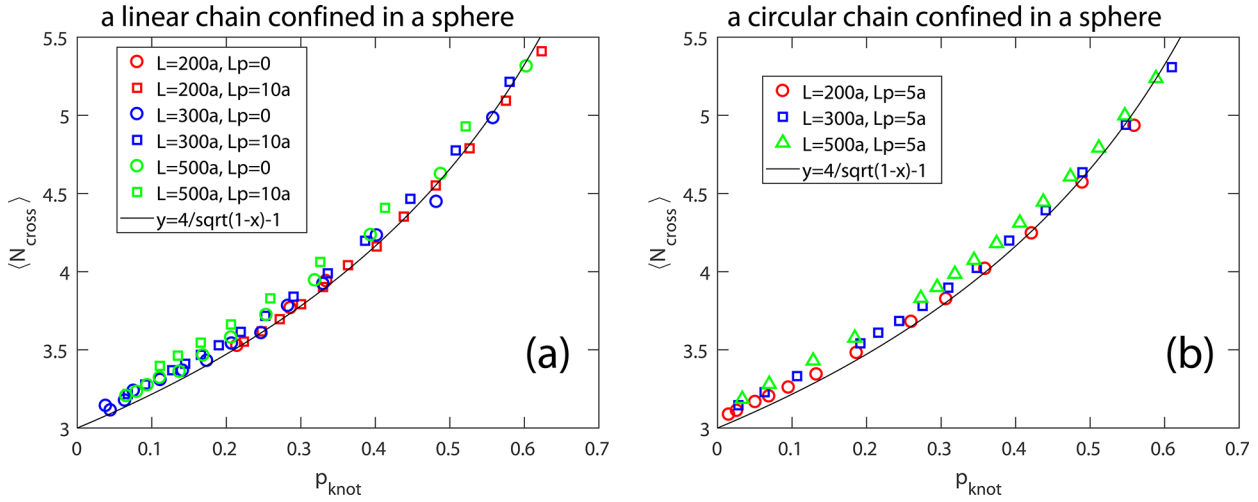

Figure 4. (a) Scatter plot of $\langle N_{cross} \rangle$ against p_{knot} using the Alexander polynomials to identify knot types. The linear polymers conformations are generated by PERM simulations. (b) Scatter plot of $\langle N_{cross} \rangle$ against p_{knot} using the Alexander polynomials to identify knot types. The circular polymers conformations are generated by Monte Carlo simulations.

Note that for a polymer with (L/a) segments, N_{cross} has an upper bound $\sim(L/a)^2$ (all segments cross others). A better fit can be obtained using

$$y = -0.0467x^2 + 0.6988x + 1.1132 \quad (2)$$

with $y = \ln(\langle N_{cross} \rangle)$ and $x = \ln(1/(1 - p_{knot}))$, as shown by the red line in Figure 3b.

3.5. Universal Knot Spectra. To understand the universal correlation, we analyze the distribution of the minimal crossing number, $P(N_{cross})$. Note that p_{knot} can be determined from the distribution of N_{cross} through

$$p_{knot} \equiv 1 - P(N_{cross} = 0) \quad (3)$$

Figure 5 shows three pairs of histograms of N_{cross}, while each pair corresponds to two simulations with different parameters

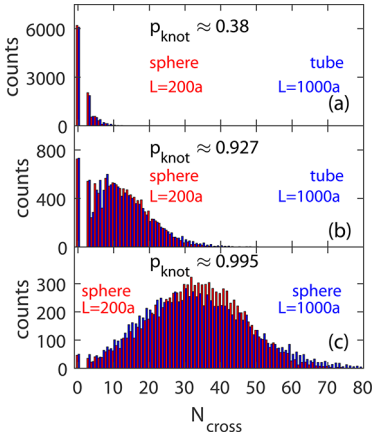

Figure 5. Distribution of N_{cross}. In each plot, the results from two simulations with similar p_{knot} are compared. All red bars correspond to $L = 200a$, $L_p = 10a$, and spherical confinement. The blue bars in (a) and (b) correspond to the polymers with $L = 1000a$ and $L_p = 10a$ in tube confinement, while the blue bars in (c) correspond to the polymer with $L = 1000a$ and $L_p = 0$ in spherical confinement.

of L, L_p, and D_{sphere} or D_{tube} but with nearly identical p_{knot} (see section S7 in the Supporting Information for the distributions of N_{cross} over a series of p_{knot}). We find that as long as p_{knot} is similar, the distribution of N_{cross} is also similar regardless of L, L_p, and D_{sphere} or D_{tube}. A notable difference in the distribution for different L is that the longer chain has a slight larger frequency at large N_{cross}. In principle, a longer chain could explore some large N_{cross} that cannot be reached by a shorter chain. However, the contribution of such difference to $\langle N_{cross} \rangle$ is so small that $\langle N_{cross} \rangle$ is insensitive to L.

3.6. Explanation of Universal Knot Spectra. Now we discuss the mechanism behind the universal behavior. The universal behavior is possibly caused by the *random* combinations of the over−under statuses of apparent crossings. We first elaborate the mechanism by an example and then discuss the relevance to the universal behavior. A knotted conformation can be mutated to another knot by switching the over−under status of a crossing (Figure 6a). For the knot 10_{165}

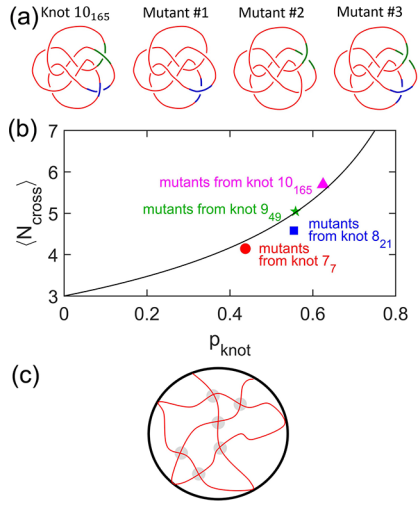

Figure 6. (a) Diagram showing mutations of the conformation of knot 10_{165} by switching the over−under statuses of one or more crossings. Mutants #1 and #2 are generated by switching the blue and green crossings, respectively, while mutant #3 corresponds to switching both. (b) Each symbol corresponds to the mutant conformations from the knot 10_{165}, 9_{49}, 8_{21}, or 7_7. The solid line is from eq 1. (c) An illustration of crossings in a confined polymer. The shadowed circles indicate the crossing points whose over−under statuses are random in an ensemble of confined polymer conformations.

DOI: 10.1021/acs.macromol.8b01340
Macromolecules 2018, 51, 6327−6333

with 10 crossings, there are 2^{10} combinations of the over−under statuses, including the knot 10_{165} itself. Our calculation of the Alexander polynomial reveals that these 1024 conformations contain 640 knotted conformations, i.e., $p_{knot} = 0.625$ with $\langle N_{cross} \rangle \approx 5.69$. Note that the Rolfsen table of knots[48] gives the Alexander polynomial for knots with $N_{cross} \leq 10$ such that we can identify the knot types of mutated conformations through the Alexander polynomials and then obtain N_{cross}. We find the pair of p_{knot} and $\langle N_{cross} \rangle$ agrees fairly well with eq 1. We have also performed such mutations for the knots 9_{49}, 8_{21}, and 7_7, and they also agree fairly well with our empirical formula (Figure 6b).

The knot type of a polymer is solely determined by the crossings on the projected conformation, such as the examples in Figure 6a. In the projection of a substantially confined polymer, the crossings mostly come from the two segments that are far apart on the contour but brought together by reflections of the confining walls (Figure 6c). This notion is consistent with the fact that a substantially confined polymer typically has orders of magnitude more apparent crossings than the same chain in the absence of confinement. The far separation along the contour and the presence of reflection points are likely to eliminate the orientational and positional correlations between two segments involved in an apparent crossing (Figure 6c). Eventually, the absence of correlations leads to the random over−under status of each apparent crossings, which results in the universal p_{knot}−$\langle N_{cross} \rangle$ relationship. We find that the polymers in free space do not follow the universal behaviors (see sections S9−S11 in the Supporting Information), which is probably because the two segments involved in a crossing are not separated by reflections of the confining walls and do not hold the random over−under status.

It is worth noting that the knotting probability and knot spectrum have been investigated previously. Koniaris and Muthumukar[50] found that the unknotting probability exponentially decays with the chain length for various strengths of excluded volume interactions. We reproduce their result in free space and find that the exponential decay disappears in confinement (see the Supporting Information). Shimamura and Deguchi[54] calculated the knot spectrum for ideal chains and obtained an apparent exponent of $\alpha_{knot} = 1.16$ in $p_{ave} \sim \exp(-\alpha_{knot} N_{cross})$ between $N_{cross} = 3$ and 8 for $L = 300a$. Here, p_{ave} is the average probability for the knots with the same N_{cross}. We reproduce the apparent exponent in free space and find the apparent exponent changes rapidly in confinement (see the Supporting Information).

3.7. Quantification of Knot Complexity by Rope Length. In addition to the crossing number, the complexity of a knot can also be described by the rope length L_{rope}, which is defined as the contour length in the tightest knot core.[55] We also find a universal correlation between the average rope length $\langle L_{rope} \rangle$ and p_{knot}. Previous studies[55,56] have proposed the relationship $L_{rope} \sim (N_{cross})^{\alpha}$ with $3/4 < \alpha < 1$, while our simulation results obtain $\alpha \approx 0.83$. See sections S5 and S6 in the Supporting Information for more details about L_{rope}.

3.8. Applications of Universal Behaviors. The universal p_{knot}−$\langle N_{cross} \rangle$ relationship discovered here is for equilibrium conformations of single confined polymers. The relationship between p_{knot} and N_{cross} may break down for confined polymers generated from nonequilibrium processes. Hence, examining whether p_{knot} and N_{cross} obey eq 1 is one method to evaluate whether the observed knots in confined polymers are from an equilibrium conformation. For example, the experiments of *E. coli* DNA in 40−50 nm nanochannels by Reifenberger et al.[31] observed a low frequency (∼7%) of possible DNA knots (or backfolds), while these possible DNA knots are rather complex with the typical rope length of ∼1700 nm, which is about 340 times a typical DNA effective diameter. Such low-frequency and complex knots are probably caused by the nonequilibrium process that drives DNA into a nanochannel or by other reasons.

The universal knot spectrum suggests an experimental approach to produce a desired knot spectrum by controlling DNA compression. Recent experiments have observed complex knots in single DNA molecules that are compressed by electric fields[12,13] or confined by nanochannels.[57] Controlling the extent of DNA compression can tune the knot spectrum that follows the universal behaviors.

The universal behaviors are also relevant to macroscale objects, for example, squeezing a headphone cable into a pocket many times and observing the knotting probability and knot complexity. In a previous study by Raymer and Smith,[5] a string with a diameter of 3.2 mm and a length from 0.46 to 6 m was tumbled inside a box with a size of 0.3 m × 0.3 m × 0.3 m. In 3415 trials, they observed about 120 different knot types with N_{cross} up to 11, and most knots are prime knots. However, these macroscale objects are out of equilibrium. Their knotting properties may not follow the universal behavior but depend on the process of generating conformations.

4. CONCLUSIONS

In conclusion, we find universal knot spectra for confined polymers, which only depend on the total knotting probability. Such universal knot spectra suggest that the knotting in confined polymers is likely to be created by random combinations of the over−under statuses of apparent crossings. The mutations of over−under status of apparent crossings also provide valuable insights into the pathways from one topological state to another and the connectivity in knot space.

Knotting becomes common for a confined polymer, and the knotting probability can rapidly approach 100% as the degree of confinement increases, even for a short polymer with hundreds of monomers. In addition, knotting (intrachain entanglement) can dramatically affect polymer behaviors, akin to how interchain entanglement affects polymer behavior, which has been addressed extensively in classic polymer physics. Hence, understanding knotting is important and inevitable for a confined polymer and also has biological implications, e.g., DNA knotting in viruses[14,15] and in chromosomes.[58−60] Considering the simple polymer model used here, the universal behaviors observed in this work may also apply for macroscopic linear objects (Figure 1a), and may be relevant to protein knots,[8−10,20,61] because the globular protein structures and confined polymers share similar compact conformations.

■ ASSOCIATED CONTENT

Supporting Information

The Supporting Information is available free of charge on the ACS Publications website at DOI: 10.1021/acs.macromol.8b01340.

Simulation details; benchmark simulations of torus and twist knots; distribution of the crossing number; further discussion about universal behaviors; comparison with the previous data by Koniaris and Muthukumar (PRL, 1991) and Shimamura and Deguchi (PRE, 2002) (PDF)

DOI: 10.1021/acs.macromol.8b01340
Macromolecules 2018, 51, 6327−6333

AUTHOR INFORMATION

Corresponding Author

*E-mail: pdoyle@mit.edu (P.S.D.).

ORCID

Liang Dai: 0000-0002-4672-6283

Patrick S. Doyle: 0000-0003-2147-9172

Notes

The authors declare no competing financial interest.

REFERENCES

(1) Turner, J.; van de Griend, P. *History and Science of Knots*; World Scientific: 1996.

(2) Ben-Naim, E.; Daya, Z. A.; Vorobieff, P.; Ecke, R. E. Knots and Random Walks in Vibrated Granular Chains. *Phys. Rev. Lett.* **2001**, *86*, 1414−1417.

(3) Belmonte, A.; Shelley, M. J.; Eldakar, S. T.; Wiggins, C. H. Dynamic Patterns and Self-Knotting of a Driven Hanging Chain. *Phys. Rev. Lett.* **2001**, *87*, 114301.

(4) Hickford, J.; Jones, R.; du Pont, S. C.; Eggers, J. Knotting probability of a shaken ball-chain. *Phys. Rev. E* **2006**, *74*, 052101.

(5) Raymer, D. M.; Smith, D. E. Spontaneous knotting of an agitated string. *Proc. Natl. Acad. Sci. U. S. A.* **2007**, *104*, 16432−16437.

(6) Arai, Y.; Yasuda, R.; Akashi, K.-i.; Harada, Y.; Miyata, H.; Kinosita, K.; Itoh, H. Tying a molecular knot with optical tweezers. *Nature* **1999**, *399*, 446−448.

(7) Bao, X. R.; Lee, H. J.; Quake, S. R. Behavior of complex knots in single DNA molecules. *Phys. Rev. Lett.* **2003**, *91*, 265506.

(8) Taylor, W. R.; Lin, K. Protein knots: a tangled problem. *Nature* **2003**, *421*, 25−25.

(9) Virnau, P.; Mirny, L. A.; Kardar, M. Intricate knots in proteins: Function and evolution. *PLoS Comput. Biol.* **2006**, *2*, e122.

(10) Kolesov, G.; Virnau, P.; Kardar, M.; Mirny, L. A. Protein knot server: detection of knots in protein structures. *Nucleic Acids Res.* **2007**, *35*, W425−W428.

(11) Rosa, A.; Di Ventra, M.; Micheletti, C. Topological jamming of spontaneously knotted polyelectrolyte chains driven through a nanopore. *Phys. Rev. Lett.* **2012**, *109*, 118301.

(12) Tang, J.; Du, N.; Doyle, P. S. Compression and self-entanglement of single DNA molecules under uniform electric field. *Proc. Natl. Acad. Sci. U. S. A.* **2011**, *108*, 16153−16158.

(13) Renner, C. B.; Doyle, P. S. Stretching self-entangled DNA molecules in elongational fields. *Soft Matter* **2015**, *11*, 3105−3114.

(14) Arsuaga, J.; Vázquez, M.; Trigueros, S.; Sumners, D. W.; Roca, J. Knotting probability of DNA molecules confined in restricted volumes: DNA knotting in phage capsids. *Proc. Natl. Acad. Sci. U. S. A.* **2002**, *99*, 5373−5377.

(15) Arsuaga, J.; Vazquez, M.; McGuirk, P.; Trigueros, S.; Sumners, D. W.; Roca, J. DNA knots reveal a chiral organization of DNA in phage capsids. *Proc. Natl. Acad. Sci. U. S. A.* **2005**, *102*, 9165−9169.

(16) Matthews, R.; Louis, A.; Yeomans, J. Knot-controlled ejection of a polymer from a virus capsid. *Phys. Rev. Lett.* **2009**, *102*, 088101.

(17) Marenduzzo, D.; Micheletti, C.; Orlandini, E.; et al. Marenduzzo, Davide and Micheletti, Cristian and Orlandini, Enzo and others Topological friction strongly affects viral DNA ejection. *Proc. Natl. Acad. Sci. U. S. A.* **2013**, *110*, 20081−20086.

(18) Christian, T.; Sakaguchi, R.; Perlinska, A. P.; Lahoud, G.; Ito, T.; Taylor, E. A.; Yokoyama, S.; Sulkowska, J. I.; Hou, Y. Methyl transfer by substrate signaling from a knotted protein fold. *Nat. Struct. Mol. Biol.* **2016**, *23*, 941−948.

(19) Marcos, V.; Stephens, A. J.; Jaramillo-Garcia, J.; Nussbaumer, A. L.; Woltering, S. L.; Valero, A.; Lemonnier, J.-F.; Vitorica-Yrezabal, I. J.; Leigh, D. A. Allosteric initiation and regulation of catalysis with a molecular knot. *Science* **2016**, *352*, 1555−1559.

(20) San Martín, Á.; Rodriguez-Aliaga, P.; Molina, J. A.; Martin, A.; Bustamante, C.; Baez, M. Knots can impair protein degradation by ATP-dependent proteases. *Proc. Natl. Acad. Sci. U. S. A.* **2017**, *114*, 9864−9869.

(21) Narsimhan, V.; Renner, C. B.; Doyle, P. S. Translocation dynamics of knotted polymers under a constant or periodic external field. *Soft Matter* **2016**, *12*, 5041−5049.

(22) Suma, A.; Micheletti, C. Pore translocation of knotted DNA rings. *Proc. Natl. Acad. Sci. U. S. A.* **2017**, *114*, E2991−E2997.

(23) Rybenkov, V. V.; Cozzarelli, N. R.; Vologodskii, A. V. Probability of DNA knotting and the effective diameter of the DNA double helix. *Proc. Natl. Acad. Sci. U. S. A.* **1993**, *90*, 5307−5311.

(24) Shaw, S. Y.; Wang, J. C. Knotting of a DNA chain during ring closure. *Science* **1993**, *260*, 533−536.

(25) Virnau, P.; Kantor, Y.; Kardar, M. Knots in globule and coil phases of a model polyethylene. *J. Am. Chem. Soc.* **2005**, *127*, 15102−15106.

(26) Grosberg, A. Y.; Rabin, Y. Metastable tight knots in a wormlike polymer. *Phys. Rev. Lett.* **2007**, *99*, 217801.

(27) Tubiana, L.; Rosa, A.; Fragiacomo, F.; Micheletti, C. Spontaneous knotting and unknotting of flexible linear polymers: equilibrium and kinetic aspects. *Macromolecules* **2013**, *46*, 3669−3678.

(28) Dai, L.; Renner, C. B.; Doyle, P. S. Metastable Tight Knots in Semiflexible Chains. *Macromolecules* **2014**, *47*, 6135−6140.

(29) Dai, L.; Renner, C. B.; Doyle, P. S. Origin of Metastable Knots in Single Flexible Chains. *Phys. Rev. Lett.* **2015**, *114*, 037801.

(30) Metzler, R.; Reisner, W.; Riehn, R.; Austin, R.; Tegenfeldt, J.; Sokolov, I. M. Diffusion mechanisms of localised knots along a polymer. *Europhys. Lett.* **2006**, *76*, 696.

(31) Reifenberger, J. G.; Dorfman, K. D.; Cao, H. Topological events in single molecules of E. coli DNA confined in nanochannels. *Analyst* **2015**, *140*, 4887−4894.

(32) Micheletti, C.; Orlandini, E. Knotting and metric scaling properties of DNA confined in nano-channels: a Monte Carlo study. *Soft Matter* **2012**, *8*, 10959−10968.

(33) Micheletti, C.; Orlandini, E. Numerical Study of Linear and Circular Model DNA Chains Confined in a Slit: Metric and Topological Properties. *Macromolecules* **2012**, *45*, 2113−2121.

(34) Micheletti, C.; Orlandini, E. Knotting and Unknotting Dynamics of DNA Strands in Nanochannels. *ACS Macro Lett.* **2014**, *3*, 876−880.

(35) Dai, L.; Renner, C. B.; Doyle, P. S. Metastable Knots in Confined Semiflexible Chains. *Macromolecules* **2015**, *48*, 2812−2818.

(36) Vologodskii, A. Brownian dynamics simulation of knot diffusion along a stretched DNA molecule. *Biophys. J.* **2006**, *90*, 1594−1597.

(37) Matthews, R.; Louis, A. A.; Likos, C. N. Effect of Bending Rigidity on the Knotting of a Polymer under Tension. *ACS Macro Lett.* **2012**, *1*, 1352−1356.

(38) Klotz, A. R.; Narsimhan, V.; Soh, B. W.; Doyle, P. S. Dynamics of DNA Knots during Chain Relaxation. *Macromolecules* **2017**, *50*, 4074−4082.

(39) Marenduzzo, D.; Orlandini, E.; Stasiak, A.; Tubiana, L.; Sumners, D. W.; Micheletti, C. DNA−DNA interactions in bacteriophage capsids are responsible for the observed DNA knotting. *Proc. Natl. Acad. Sci. U. S. A.* **2009**, *106*, 22269−22274.

(40) D'Adamo, G.; Micheletti, C. Molecular Crowding Increases Knots Abundance in Linear Polymers. *Macromolecules* **2015**, *48*, 6337−6346.

(41) Dai, L.; Doyle, P. S. Effects of Intrachain Interactions on the Knot Size of a Polymer. *Macromolecules* **2016**, *49*, 7581−7587.

(42) Grassberger, P. Pruned-enriched Rosenbluth method: Simulations of θ polymers of chain length up to 1 000 000. *Phys. Rev. E: Stat. Phys., Plasmas, Fluids, Relat. Interdiscip. Top.* **1997**, *56*, 3682.

(43) Dai, L.; van der Maarel, J.; Doyle, P. S. Extended de Gennes Regime of DNA Confined in a Nanochannel. *Macromolecules* **2014**, *47*, 2445−2450.

(44) Plimpton, S. Fast parallel algorithms for short-range molecular dynamics. *J. Comput. Phys.* **1995**, *117*, 1−19.

(45) Dai, L.; Jones, J. J.; van der Maarel, J. R.; Doyle, P. S. A systematic study of DNA conformation in slitlike confinement. *Soft Matter* **2012**, *8*, 2972−2982.

DOI: 10.1021/acs.macromol.8b01340
Macromolecules 2018, 51, 6327−6333

(46) Dai, L.; Renner, C. B.; Doyle, P. S. The polymer physics of single DNA confined in nanochannels. *Adv. Colloid Interface Sci.* **2016**, *232*, 80−100.
(47) Dai, L.; Doyle, P. S. Trapping a Knot into Tight Conformations by Intra-Chain Repulsions. *Polymers* **2017**, *9*, 57.
(48) Rolfsen, D. *Table of Knots and Links*; Publish or Perish Press: Wilmington, DE, 1976; Appendix C in Knots and Links.
(49) Micheletti, C.; Marenduzzo, D.; Orlandini, E. Polymers with spatial or topological constraints: Theoretical and computational results. *Phys. Rep.* **2011**, *504*, 1−73.
(50) Koniaris, K.; Muthukumar, M. Knottedness in ring polymers. *Phys. Rev. Lett.* **1991**, *66*, 2211.
(51) Micheletti, C.; Marenduzzo, D.; Orlandini, E.; Sumners, D. Simulations of knotting in confined circular DNA. *Biophys. J.* **2008**, *95*, 3591−3599.
(52) Dai, L.; van der Maarel, J. R.; Doyle, P. S. Effect of nanoslit confinement on the knotting probability of circular DNA. *ACS Macro Lett.* **2012**, *1*, 732−736.
(53) Jain, A.; Dorfman, K. D. Simulations of knotting of DNA during genome mapping. *Biomicrofluidics* **2017**, *11*, 024117.
(54) Shimamura, M. K.; Deguchi, T. Knot complexity and the probability of random knotting. *Phys. Rev. E: Stat. Phys., Plasmas, Fluids, Relat. Interdiscip. Top.* **2002**, *66*, 040801.
(55) Katritch, V.; Bednar, J.; Michoud, D.; Scharein, R. G.; et al. Katritch, Vsevolod and Bednar, Jan and Michoud, Didier and Scharein, Robert G and others Geometry and physics of knots. *Nature* **1996**, *384*, 142.
(56) Buck, G. Four-thirds power law for knots and links. *Nature* **1998**, *392*, 238−239.
(57) Amin, S.; Khorshid, A.; Zeng, L.; Zimny, P.; Reisner, W. A nanofluidic knot factory based on compression of single DNA in nanochannels. *Nat. Commun.* **2018**, *9*, 1506.
(58) Grosberg, A.; Rabin, Y.; Havlin, S.; Neer, A. Crumpled globule model of the three-dimensional structure of DNA. *EPL (Europhys. Lett.)* **1993**, *23*, 373.
(59) Mirny, L. A. The fractal globule as a model of chromatin architecture in the cell. *Chromosome Res.* **2011**, *19*, 37−51.
(60) Lieberman-Aiden, E.; Van Berkum, N. L.; Williams, L.; Imakaev, M.; Ragoczy, T.; Telling, A.; Amit, I.; Lajoie, B. R.; Sabo, P. J.; Dorschner, M. O.; et al. Lieberman- Aiden, Erez and Van Berkum, Nynke L and Williams, Louise and Imakaev, Maxim and Ragoczy, Tobias and Telling, Agnes and Amit, Ido and Lajoie, Bryan R and Sabo, Peter J and Dorschner, Michael O and others Comprehensive mapping of long-range interactions reveals folding principles of the human genome. *Science* **2009**, *326*, 289−293.
(61) Ziegler, F.; Lim, N. C.; Mandal, S. S.; Pelz, B.; Ng, W.-P.; Schlierf, M.; Jackson, S. E.; Rief, M. Knotting and unknotting of a protein in single molecule experiments. *Proc. Natl. Acad. Sci. U. S. A.* **2016**, *113*, 7533−7538.

DOI: 10.1021/acs.macromol.8b01340
Macromolecules 2018, 51, 6327−6333